COMPEL—The International Journal for Computation and Mathematics in Electrical and Electronic Engineering
Vol. 14, No. 2/3, 139–156 © 1995 MCB University Press Ltd

'A POSTERIORI' ERROR INDICATOR AND ERROR ESTIMATORS FOR ADAPTIVE MESH REFINEMENT

K.C. CHELLAMUTHU and NATHAN IDA
Department of Electrical Engineering, The University of Akron, OH 44325-3904, USA

(Received 1995)

ABSTRACT: Two different *'a posteriori'* error estimation techniques are proposed in this paper. The effectiveness of the error estimates in adaptive mesh refinement for 2D and 3D electrostatic problems are also analyzed with numerical test results. The post-processing method employs an improved solution to estimate the error, whereas the gradient of field method utilizes the gradient of the field solution for estimating the *'a posterior'* error. The gradient of field method is computationally inexpensive, since it solves a local problem on a patch of elements. The error estimates are tested by solving a set of self-adjoint boundary value problems in 2D and 3D using a hierarchical minimal tree based mesh refinement algorithm. The numerical test results and the performance evaluation establish the effectiveness of the proposed error estimates for adaptive mesh refinement.

I INTRODUCTION

The most crucial part of an adaptive FE computation is the availability of an efficient and reliable error estimation technique to predict accurately the error in the solution. In order to improve the solution accuracy it is necessary to identify the inherent error involved in the discretization process of a FE method. Many heuristic error estimation strategies have been proposed in the past. Error estimates can be broadly clasified into two viz, *'a posterior'* and *'a priori'*. Most of the practically usable error estimates are of an *'a posterior'* type. It is very difficult to estimate the quantity and quality of errors *'a priori'*. This is due to the fact that the information available before the solution process may be insufficient to accurately estimate the error.

An *'a posteriori'* error estimation provides two vital parameters viz, error indicator and error estimator. An error indicator is a value in some norm which identifies the elements having the largest errors for mesh refinement. On the other hand an error estimator is a global measure of error acting as a stopping criterion to determine the level of refinement necessary to achieve the desired solution accuracy. It is computed from the error indicator and the local error information through the summable squares of an appropriate norm.

A *posteriori* error indicators provide not only information on the quality and quantity of error distribution but also provide means for practical mesh optimization. In order to compute efficient and reliable error bounds, an *'a posteriori'* error estimate uses all the information available during the solution process. Some *'a posteriori'* error

estimates bound the true error by approximating the error in the solution. Most error estimates provide an asymptotic rate of convergence as the mesh size is reduced ($h_{max} \to 0$) or the degrees of the approximating polynomial ($p \to \infty$) is increased. A good error indicator will be able to locate exactly the regions of the problem domain which need more refinement to reduce the error. It controls the adaptive process in order to generate nearly optimal meshes. In an optimal mesh the error is equi-distributed among all the elements and all the error indicators will be asymptotically equal.

An efficient error indicator should be computationally inexpensive and should be simple to implement. Also it should be reliable and must be independent of the type and class of problems solved. An error estimate should also operate uniformly on different material types. In addition to controlling the mesh adaptation, an error indicator should help to assess the reliability of the method employed.

Many strategies utilizing the residual as the primary field quantity for error estimation are available [1–6]. These are based on the fact that the insufficient satisfaction of the governing differential equation leads to estimation of errors in the solution. This has been a successful error estimation technique in many problems in structural mechanics, fluid dynamics and electromagnetics. In particular, in linear elliptic boundary value problems employing odd degree polynomial approximation, by minimizing the residual, it is possible to achieve a faster rate of convergence. The post-processing method of error estimation employs the solution function, its derivatives or both to estimate the error. This strategy has also been widely used for adaptive FE application in fluid flow problems, structural dynamics and electromagnetics [7–11]. The dual energy method involves solving primal and dual problems providing an energy bound for the solution error. Although the method is computationally very expensive it has been applied to solve many adaptive problems in structural engineering and electromagnetics [12–14]. Other types of *'a posteriori'* error estimation procedures utilize the characteristics and continuity conditions of the field parameters to estimate the error.

The efficiency of *'a posteriori'* error estimates depends on the availability of reliable information. Since an adaptive FE mesh is an optimal feedback procedure, the error estimate should introduce as few degrees of freedom as possible during the mesh refinement. Another important aspect of error estimation is that it should provide an efficient smoothing of the solution in the vicinity or at points of singularity. Singularities may be divided into two categories viz, geometrical singularities and problem singularities. Geometric singularities include sharp bends, re-entrant corners and curved boundaries and the natural problem singularities involve irregular and abrupt variation of the solution due to shocks.

Two *'a posteriori'* error estimation schemes are discussed in this paper. In the first method, solutions obtained for two successive adaptive meshes along with interpolation are used to compute the error. In the second method the error is computed as the gradient of the solution by solving a local problem. The effectiveness of the two error estimates are verified by solving electrostatic problems in 2D and 3D. The paper is organized as follows. In the first part of the paper, the methodology and theory employed to compute the *'a posteriori'* error using post-processing and gradient of field method of error estimation is presented. The numerical case studies and the performance evaluation of both error estimators are analyzed in the second part of the paper.

A Error analysis

In order to assess the efficiency and reliability of an error estimation technique, it is necessary to provide a detailed mathematical study and analysis of errors and error measures. To establish a mathematical analysis, we define an abstract boundary value problem for a weak Galerkin formulation in 2D and 3D as follows,

Let Ω be a smooth bounded domain $\Omega \subset R^n$ where $n = 2, 3$ with boundary $\Gamma = d\Omega = \Gamma_\phi \cup \Gamma_\alpha$ consisting of two disjoint sections Γ_ϕ and Γ_α such that $\Gamma_\phi \cap \Gamma_\alpha = \phi$ on which we seek to find the solution Φ, then the problem is,

$$-\Delta\Phi = f \text{ in } \Omega$$

$$\Phi = \Phi_0 \text{ on } \Gamma_\phi$$

$$\frac{\partial\Phi}{\partial n} = g \text{ on } \Gamma_\alpha \tag{1}$$

Assuming that the solution Φ lies in the Sobolev space $H^1(\Omega)$ and let $V(\Omega)$ be the corresponding Hilbert space containing all the admissible finite dimensional subspaces of the trial functions used to approximate the solution. Associating a bilinear coercive and continuous form $B(.,.)$, it is possible to prove that this class of linear self adjoint positive definite problems satisfies the consistency conditions and the convergence theorem. This establishes the uniqueness and existence of the solution to this class of problems [15–16]. The satisfaction of the consistency condition is necessary for verifying the effectiveness of the error estimate. This is due to the fact that the approximate solution of a FE method converges to a true solution in the sense of a global energy in some norm. As the solution converges, the error in the solution also converges to the true error in some norm measured as a local quantity of error.

The basic theory of FE approximation is based on satisfying the consistency conditions such as completeness and continuity of solutions. The well-posedness of a problem involving the existence and uniqueness of an exact and approximate solution and the guarantee of convergence allows estimation of the error in a more reliable way. This leads to the application of a rigorous mathematical and functional analysis to the error estimation and application of these techniques to automatic adaptive FE methods.

All elliptic boundary value problems possessing the property of linear self-adjoint positive definiteness should satisfy the following set of consistency conditions in order to achieve an asymptotic convergence of the solution:

- For a well-posed problem:
  - The problem has a solution (existence).
  - Exact and approximate solutions to the problem exist (uniqueness property).
- The solution should vary continuously as a function of input variables.
- For a linear self adjoint positive definite differential operator, trial functions should satisfy the appropriate completeness and continuity conditions to ensure that a sequence of approximate solutions converge to an exact solution.

II POST-PROCESSING AND INTERPOLATION METHOD OF ERROR ESTIMATION

Computing the post-processed field quantities from an approximated solution is simple and inexpensive in most cases. The post-processed data may be an improved version of the solution, the gradient of the solution or the higher order derivatives. Based on the rapid convergence effect of the solution at some special points in the mesh compared to other points, superconvergent techniques have been developed for estimating the error [7–9]. Post-processing techniques involve methods such as the use of numerical quadrature points to compute certain field quantities, averaging or smoothing procedures based on projection techniques, extraction procedures and iterative refinement methods.

In the proposed post-processing technique, the improved solution is used for error estimation. In this approach, the local error on each element is computed as the difference between the approximated solutions from two consecutive adaptive meshes using a mesh halving procedure. The method can be mathematically represented as follows,

Let $M_i(\Omega)$ and $M_j(\Omega)$ be the two successive admissible adaptive meshes. Mesh $M_j(\Omega)$ is the superset of mesh $M_i(\Omega)$ such that $M_i(\Omega) \subset M_j(\Omega)$ and $M_i(\Omega)$ is halved to generate mesh $M_j(\Omega)$ *i.e* each element (quadrilateral in 2D and hexahedral in 3D) is divided into four elements in 2D and eight elements in 3D. The solution at each mid edge of the element in the unrefined mesh $M_i(\Omega)$ is interpolated using the original solution and the interpolated new solution is obtained as Φ_i. The improved solution is obtained by using the refined mesh $M_j(\Omega)$. Since the solution at each node including the interpolated node in the first mesh $M_i(\Omega)$ is solved using the refined mesh, the solution Φ_j will obviously be an improved solution for the corresponding element.

The absolute error e is computed from the difference between the two solutions Φ_i and Φ_j. The absolute error on each element will not indicate to what extent the approximated solution deviates from the exact solution in the sense of a global convergence and so it is necessary to use some suitable norms to measure the error. Since the approximated solution converges to the true solution in the global energy sense, the use of an energy norm is more appropriate and natural. Although different norms to measure the deviation of the approximated solution from the actual solution can be used, the L_2 norm has an advantage in that it can be associated with any quantity. An L_2 norm is a dimensionless scalar quantity and can be used to represent the error in the energy of the system.

A Error measures

The following are the different error measures used in the post-processing error estimation. The computed absolute error is $e = |\Phi_{ex} - \Phi_i|$ where Φ_{ex} and Φ_i are exact and approximate solutions respectively. Using the L_2 norm, the error in each element can be represented as follows:

$$\|e_i\|_{L_2} = \left\{ \int_\Omega e^T e \, d\Omega \right\}^{\frac{1}{2}} \tag{2}$$

The relative percentage error for each element in L_2 norm is,

$$\eta_i = \{\|e\|/\|\Phi_{ex}\|\}*100\% \tag{3}$$

Adding the error and the approximate solution, the relative percentage error in each element is,

$$\eta_i = \{\|e_i\|/(\|\Phi\|^2 + \|e_i\|^2)^{\frac{1}{2}}\}*100\% \tag{4}$$

The relative percentage error η_i is used as the local elementwise error indicator to identify elements having large errors. Using the global measure of error e_t the estimator in relative percentage error can be computed as follows:

$$\|e_t\|_{L_2} = \left\{\sum_{i=1}^{N} \|e_i\|_{L_2}^2\right\}^{\frac{1}{2}} \tag{5}$$

$$\eta_T = \left\{\|e_t\|_{L_2}/\left[\sum_{i=1}^{N} \|\Phi_i\|^2 + \|e_t\|_{L_2}^2\right]^{\frac{1}{2}}\right\}*100\% \tag{6}$$

The refinement criterion is fixed using the elementwise relative percentage error and the error estimator η_T. An element is marked for refinement whenever $\eta_i \geq \eta_T$. This relationship is based on the fact that an element with a large local error will contribute more to the global error than an element with small error. The overall accuracy of the solution is determined by the error estimator. The stopping criterion for the mesh is based on the global relative percentage error compared to the specified global relative percentage error η_s. The mesh refinement continues as long as $\eta_T \geq \eta_s$.

III GRADIENT OF FIELD METHOD OF ERROR ESTIMATION

In a singular region of a problem domain, one cannot expect to have a very smooth solution. Naturally the gradient of the field or flux will be highest at the singular regions of the problem where the rate of variation of the solution is larger than other regions. This is the basic idea behind the gradient of field error estimate. The improved gradient of the solution is computed by solving a local problem on a patch of elements forming a subdomain connected to each node of the element in question. The patch contains all the elements connected to each of the nodes under consideration. The error in the gradient is computed as the difference between the gradient from the local problem and the gradient of the original solution. The gradient itself or the error in the gradient can be used as a criterion for the local as well as global error estimation. The error in the gradient of a particular element acts as a good error indicator for identifying elements for refinement. The global error estimator is computed using the elementwise local error indicator. The mathematical derivation of the gradient of field error estimate is as follows,

Let g_{ex} and g be the gradient in the exact solution Φ_{ex} and the approximated solution Φ respectively and let e_g be the error in the gradient, *i.e* $e_g = |g - g_{ex}|$. Let $\tilde{g}$ be the gradient of the solution on an element computed from the local problem employing

the same approximation function which is used to approximate the solution Φ. In the case of a linear first order approximation, the derivative or the gradient of the solution g must be constant in a given element. Because g is discontinuous across neighboring elements it is a poor approximation to the true value of the gradient g_{ex}. To improve the approximation of the true gradient value, the gradient at each nodal point $\bar{g}$ is computed using the local problem formulation. The local problem involves finding the improved gradient by means of an averaging technique. This is based on the fact that nodal values are heavily influenced by changes in the field quantities of neighboring elements. A simple averaging technique is used to implement the error estimator in the proposed method. This method is simple and easy to implement, and is computationally inexpensive compared to other methods.

Let $g_{ex} = \nabla\Phi_{ex}$ and $g = \nabla\Phi$ and so the true error in the gradient is $e_g = |\nabla\Phi_{ex} - \nabla\Phi|$. Let $\bar{g}_x$ and $\bar{g}_y$ be the x and y components of the nodal derivatives of the solution computed from the local problem. Using the same approximation function the x and y component of the improved gradient can be interpolated for the element:

$$\tilde{g}_x = N\bar{g}_x \text{ and } \tilde{g}_y = N\bar{g}_y \tag{7}$$

Now the improved gradient is $\tilde{g} = \{\tilde{g}_x^2 + \tilde{g}_y^2\}^{\frac{1}{2}}$. The error in the gradient is represented as follows,

$$e_g = \{[g_x - \tilde{g}_x]^2 + [g_y - \tilde{g}_y]^2\}^{\frac{1}{2}} \tag{8}$$

and this can be explained as follows,

$$e_g = \{(e_{gx})^T(e_{gx}) + (e_{gy})^T(e_{gy})\}^{\frac{1}{2}} \text{ where } e_{gx} = |g_x - \tilde{g}_x| \text{ and } e_{gy} = |g_y - \tilde{g}_y| \tag{9}$$

The elementwise gradient error (local) in L_2 norm can be computed using the above result as,

$$\|e_{gi}\|^2 = \int_{\Omega_i} \{(e_{gx})^T(e_{gx}) + (e_{gy})^T(e_{gy})\} d\Omega \tag{10}$$

The global error norm of the gradient is,

$$\|e_g\|_{L_2} = \left\{\sum_{i=1}^{N} \|e_{gi}\|_{L_2}^2\right\}^{\frac{1}{2}} \tag{11}$$

Using the total and exact gradient error, the global relative percentage error can be computed as,

$$\eta_T = \{\|e_g\|/\|g_{ex}\|\} * 100\% \tag{12}$$

For most problems, it is difficult to find the actual solution. Hence by adding the error to the approximate solution an improved solution which is close enough to a true solution can be obtained. Using the computed gradient from the local error problem, the actual gradient may be approximated by adding the error in the gradient with the values of the computed gradient. Then the relative percentage error can be written as,

$$\eta_T = \left\{ \|e_{gi}\|_{L_2} / \left[\sum_{i=1}^{N} \|g_i\|^2 + \|e_{gi}\|_{L_2}^2 \right]^{\frac{1}{2}} \right\} * 100\% \tag{13}$$

Where $\|g_i\|_{L_2}^2 = \int_{\Omega_i} g_i^2 d\Omega$ and $\|g_{ex}\|_i^2 \approx \|g_i\|^2 + \|e_{gi}\|^2$, $i = 1, N$

By using a specified maximum allowable relative percentage error η_s, it is possible to establish a relation between the computed relative error and the specified error. This empirical relation can be used as an error indicator for mesh refinement. The element will be refined whenever $\eta_i \geq \eta_T$. In this case, the global relative error η_T helps to meet the user specified error tolerance and is useful in deciding the level of refinement necessary whereas the local relative error in some elements may be very high. Under these conditions it becomes necessary to adjust the maximum allowable error in an element using the following equation,

$$\|e_{gi}\| \leq \eta_T \left[\left\{ \sum_{i=1}^{N} \|g_i\|^2 + \|e_{gi}\|_{L_2}^2 \right\} / N \right]^{\frac{1}{2}} = e_a \tag{14}$$

Now a more reliable error criterion for elementwise refinement can be obtained as follows,

$$\zeta_i = \frac{\|e_{gi}\|_{L_2}}{e_a} \tag{15}$$

Using the above error measure, it is possible to identify the elements for refinement. For $\zeta_i < 1$ larger elements can be used for refinement since the allowable maximum error is larger and for $\zeta_i > 1$ smaller elements need be utilized for refinement. Using the size of the current element and the values of the refinement ratio ζ_i, it is possible to determine the size of an element to be refined.

IV NUMERICAL TEST RESULTS AND PERFORMANCE ANALYSIS OF ERROR ESTIMATES

The above error estimates are applied on a linear self adjoint boundary value problem in 2D and an electrostatic problem in 3D. The 2D problem is a common L-shaped domain with a corner singularity in the form of $r^{\frac{2}{3}} \sin\frac{2}{3}\theta$ where r and θ are polar coordinates. The presence of this corner singularity influences the convergence rate of the solution. Due to the pollution effect of this singularity, it will introduce error in the solution in other regions of the domain. In order to reduce this effect, elements around the corner must be refined more than in other regions. In this investigation, the error estimate is applied and a hierarchical tree based data structure with a *one-level* rule is used for mesh refinement [17]. The mesh refinement algorithm generates a smooth mesh which has a gradual transition from fine mesh near the re-entrant corner to a coarse mesh of larger elements away from the singular region. The refinement was initiated with an initial coarse mesh of 12 first order quadrilateral elements. Figure 1 shows the L-shaped domain with appropriate boundary conditions. Figure 2 and

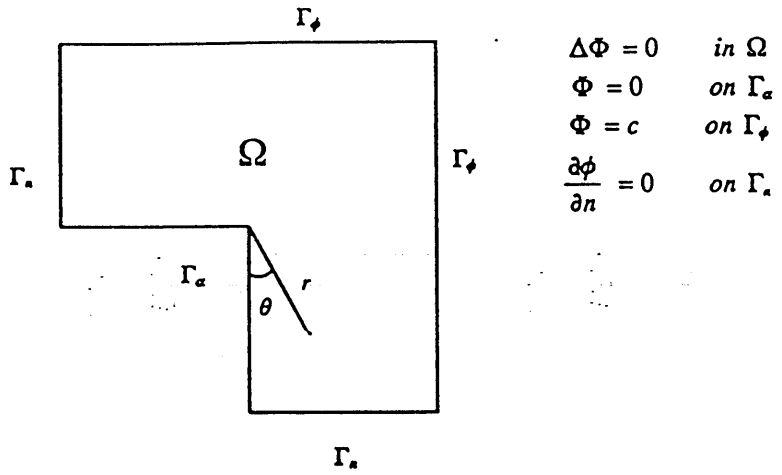

Figure 1 L-Shaped Domain.

Figure 3 show the sequence of adaptive meshes and the corresponding equi-potential plots of the solution for the post-processing error estimate. Figure 4 shows the convergence plot indicating the relation between the relative percentage error and the number of degrees of freedom.

The post-processing error estimate generates a nearly optimal mesh. As shown in Figure 2(d) the solution converges in the fourth level of refinement with 306 elements having 369 degrees of freedom. The corresponding contour plot in Figure 3(d) shows a smooth curve which is an indication of the convergence of the solution to the required accuracy. The interpretation of the optimal quality of the solution is also verified by the error convergence plot shown in Figure 4. The numerical test results for the post-processing error estimate are presented in Table 1. The above results show that the mesh is nearly optimal at this refinement level. For the purpose of verification and for the sake of completeness, additional levels of refinement were added and the adaptive meshes and the corresponding solution plots are also shown. The gradient of field method is tested on the same problem. The sequence of adaptive meshes and the corresponding equi-potential contour plots are presented in the Figure 5 and Figure 6 respectively. Table 2 shows the numerical test results for the gradient of field method of error estimation. Almost the same level of solution accuracy is achieved for this problem using the gradient of field method of error estimation with only 126 elements and 167 degrees of freedom in the fourth level of mesh refinement. A nearly optimal mesh is obtained with fewer degrees of freedom compared to the post-processing method. As can be seen from the adaptive meshes in Figure 5, the refinement is mostly concentrated near the re-entrant corner as expected. The adaptive mesh and the corresponding flux plots show the superior performance of this method over the post-processing approach. Figure 7 shows the asymptotic convergence plot of global effectivity indices for post-processing and gradient error estimates. The asymptotic convergence plot indicates that the post-processing method under estimates the error in the solution whereas the gradient of field method over estimates the error. Since effectivity index is a good measure of error leading to the convergence of the solution an asymptotic convergence helps establish the reliability of the method employed.

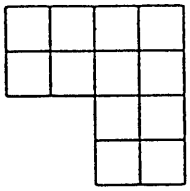

Initial Coarse Mesh – 12 Elements
Figure – 2a

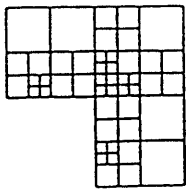

Second Level Refinement – 48 Elements
Figure 2b

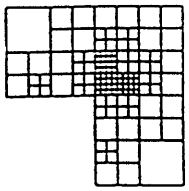

Third Level Refinement – 120 Elements
Figure – 2c

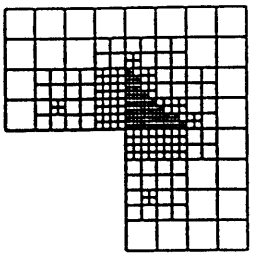

Fourth Level Refinement – 306 Elements
Figure – 2d

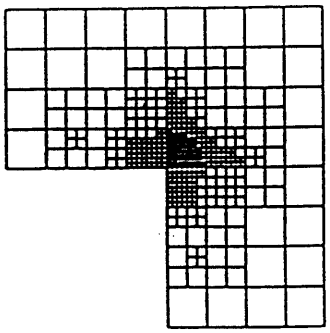

Fifth Level Refinement – 534 Elements
Figure – 2e

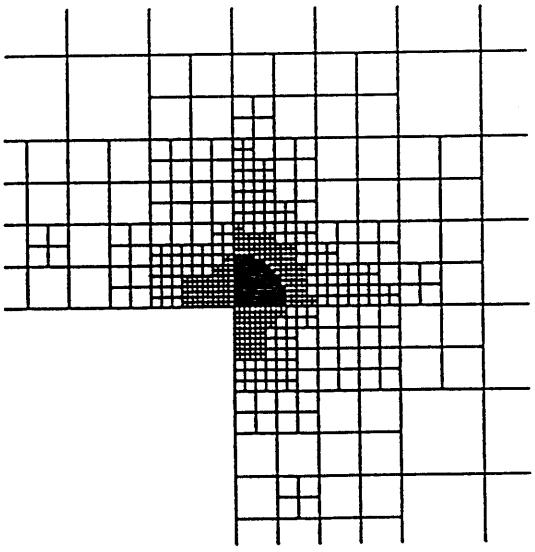

Sixth Level Refinement – 891 Elements
Figure – 2f

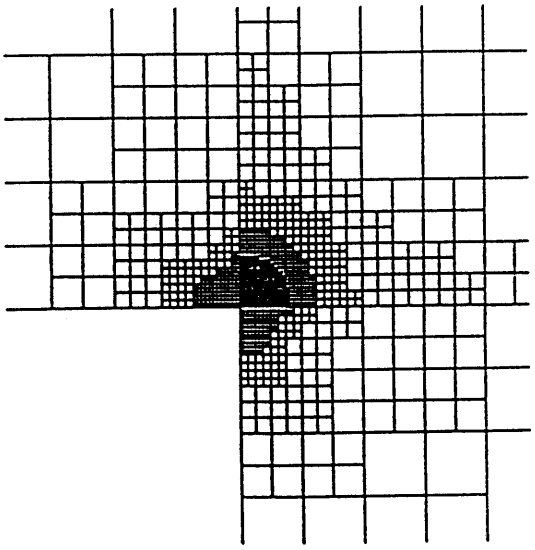

Seventh Level Refinement – 1491 Elements
Figure – 2g

Figure 2 Sequence of Adaptive Meshes on an L Shaped Domain (Post-Processing Error Estimate).

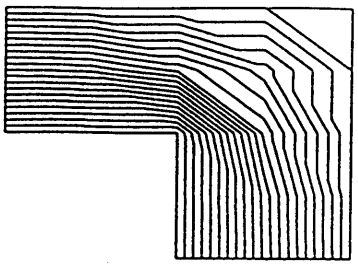

Coarse Mesh – 12 Elements
Figure – 3a

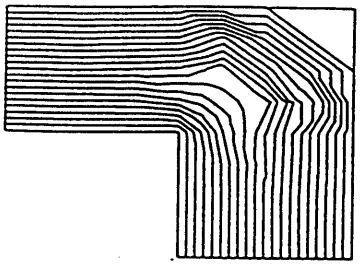

Level II – 48 Elements
Figure – 3b

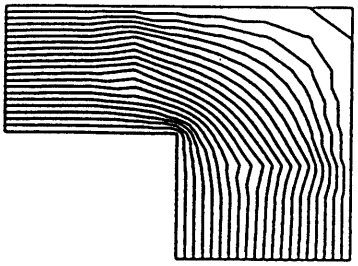

Level III – 120 Elements
Figure – 3c

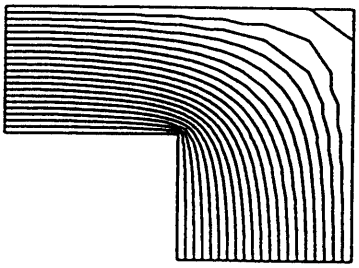

Level IV – 306 Elements
Figure – 3d

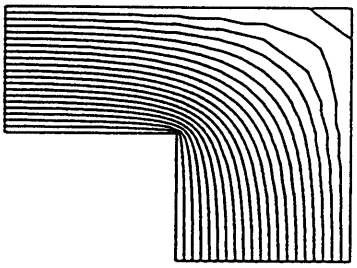

Level V – 534 Elements
Figure – .3e

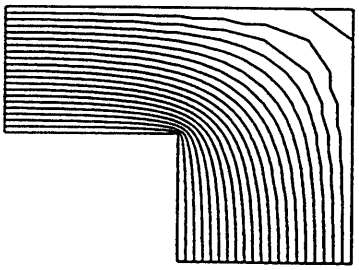

Level VI – 891 Elements
Figure – 3f

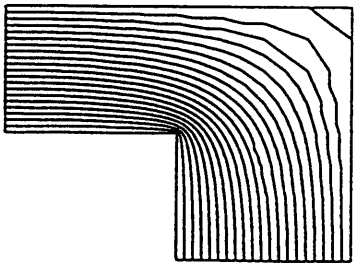

Level VII – 1491 Elements
Figure – 3g

Figure 3 Sequence of Adaptive Contour Plots on an L Shaped Domain (Post-Processing Error Estimation Method).

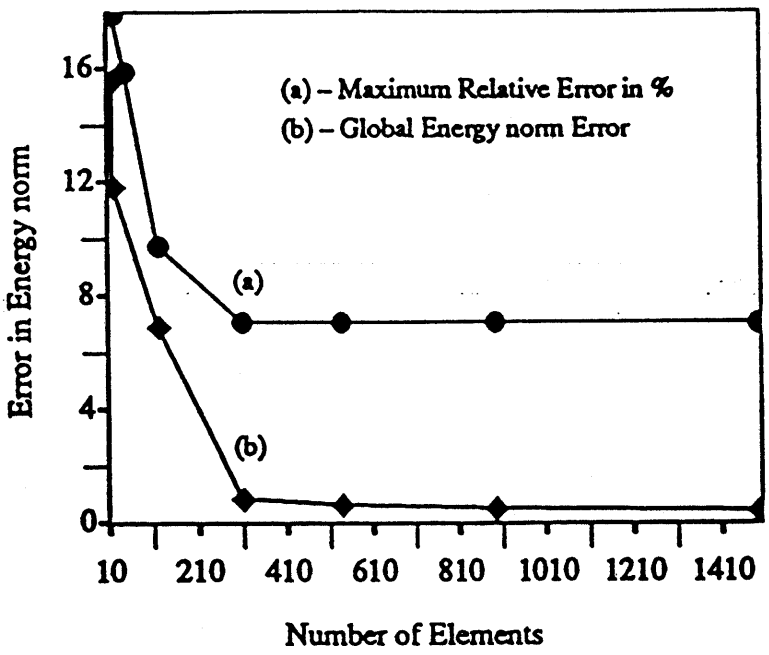

Figure 4 Error Convergence Plot for Post-Processing Method.

Table 1 Numerical Test data for Post-processing Error Estimate

Mesh number	No. of elements	Max. relative error %	Global relative error	Global energy norm $\|e\|$	Global effectivity index
1	21	17.925	6.8762	15.634	0.8208
2	48	15.8911	5.0606	11.8287	0.8535
3	120	9.7408	2.2487	6.9199	0.8813
4	306	7.0493	0.2047	0.8497	0.9104
5	534	7.0422	0.1548	0.6392	0.9727
6	891	7.0424	0.1233	0.5085	0.9817
7	1491	7.0401	0.0988	0.4244	0.9999

Table 2 Numerical Test data for Gradient of field Error Estimate

Mesh number	No. of elements	No. of nodes	Global effectivity index
1	21	34	1.0867
2	30	47	1.1384
3	39	60	1.1676
4	126	167	0.9997
5	192	245	0.9998
6	309	378	0.9996
7	489	578	0.9998
8	759	872	0.9999

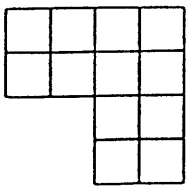

Coarse Mesh – 12 Elements
Figure – 5a

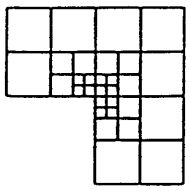

Level II – 30 Elements
Figure – 5b

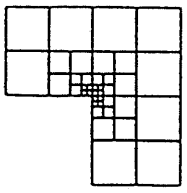

Level III – 39 Elements
Figure – 5c

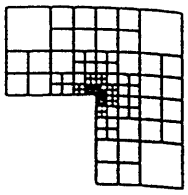

Level IV – 126 Elements
Figure – 5d

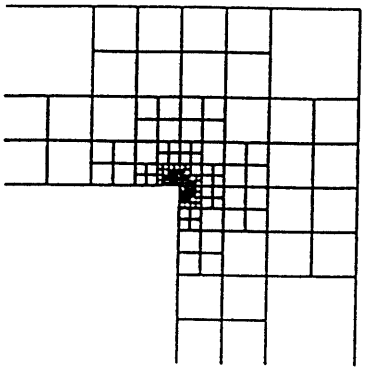

Level V – 192 Elements
Figure – 5e

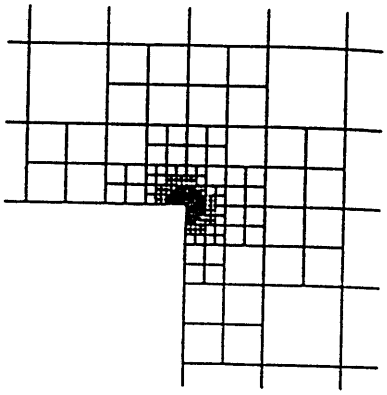

Level VI – 309 Elements
Figure – 5f

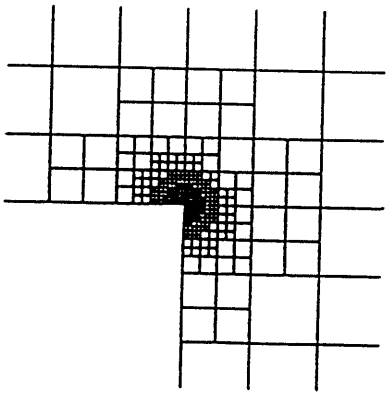

Level VII – 489 Elements
Figure – 5g

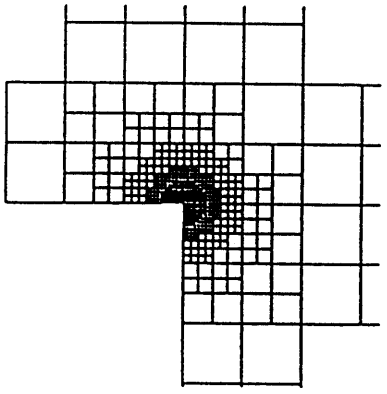

Level VIII – 759 Elements
Figure – 5h

Figure 5 Sequence of Adaptive Meshes on an L Shaped Domain (Gradient Error Estimation Method).

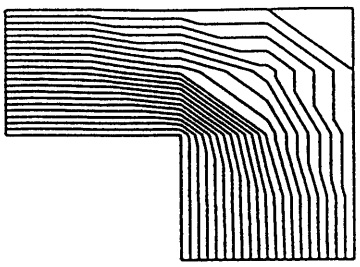

Coarse Mesh – 12 Elements
Figure – 6a

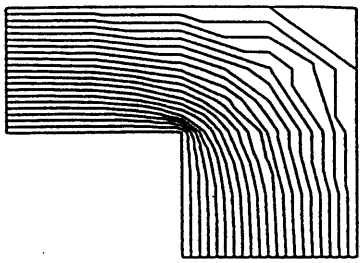

Level II – 30 Elements
Figure – 6b

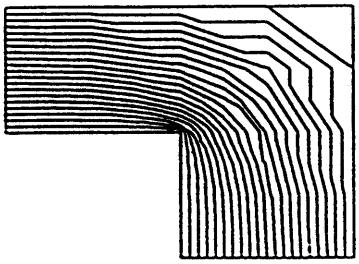

Level III – 39 Elements
Figure – 6c

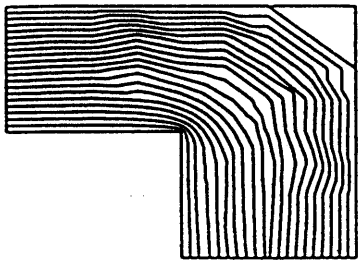

Level IV – 126 Elements
Figure – 6d

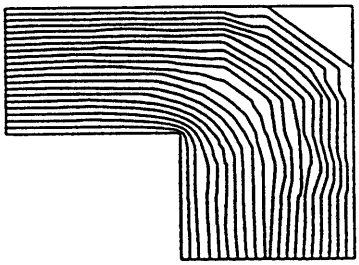

Level V – 192 Elements
Figure – 6e

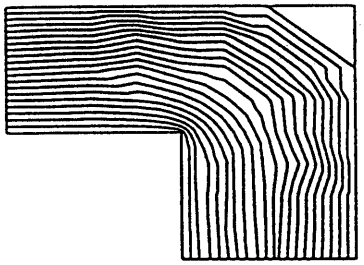

Level VI – 309 Elements
Figure – 6f

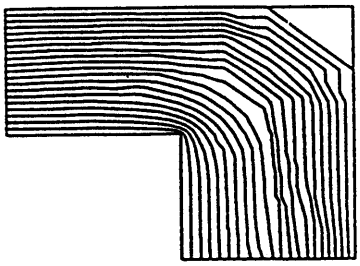

Level VII – 489 Elements
Figure – 6g

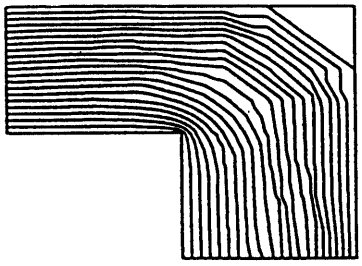

Level VIII – 759 Elements
Figure – 7.6h

Figure 6 Sequence of Adaptive Solution Plots on an L Shaped Domain (Gradient Error Estimation Method).

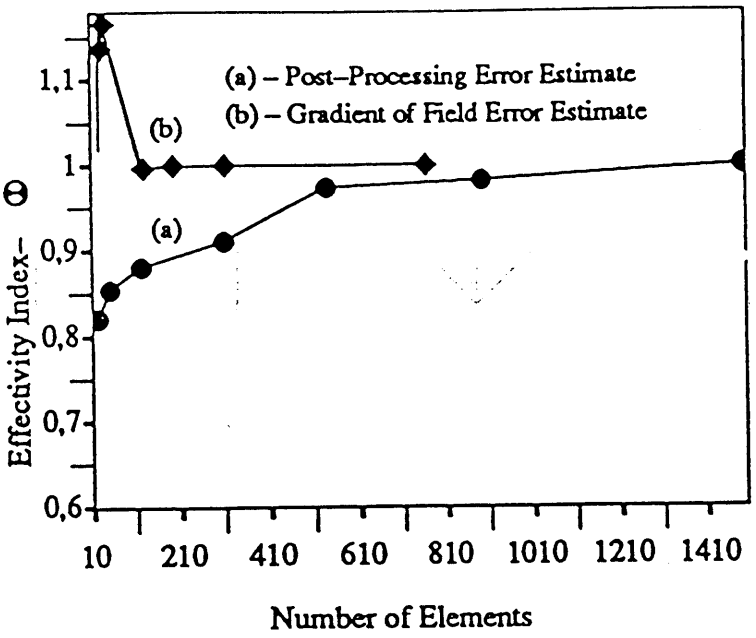

Figure 7 Asymptotic Convergence Plot of Effectivity Index.

V PERFORMANCE ANALYSIS OF ERROR ESTIMATES

The gradient of field error estimate generates a mesh following the *one-level* rule of adaptive mesh refinement algorithm. The mesh has a gradual transition from the singular region to the nonsingular region of the domain. The performance of the error indicator to refine the local elements based on the estimated error indicates that most elements with large errors in the singular regions are refined. In order to generate a graded mesh, the adjacent neighboring elements are also refined following the *one-level* rule. The algorithm along with the error indicator generates a geometrically graded mesh towards the singularity. Additional number of adaptive mesh sequences shown in the figures indicate that after obtaining the nearly optimal mesh, the errors are equi-distributed and further refinement will not contribute a significant improvement in the solution accuracy.

The post-processing and gradient of field error estimates are also applied to solve 3D electrostatic problems with two different geometries. The first problem involves finding the potential distribution inside a cube and the second problem is a 3D version of the L-section problem. The first problem was initiated with a coarse mesh of $2 \times 2 \times 2$ elements in a cube of $1 \times 1 \times 1$ units dimension with conducting boundaries. The mesh refinement algorithm in [17] employs first order isoparametric hexahedral elements. The sequence of adaptive meshes are shown in Figure 8 for the post-processing error estimate and in Figure 9 for the gradient of field method of error estimate. Since the post-processing error estimate provides a very slow rate of convergence of the approximate solution to the true solution, a larger number of degrees of freedom are required to achieve the needed accuracy in the solution.

Due to the imposed Dirichlet boundary condition on the upper plane of the cube,

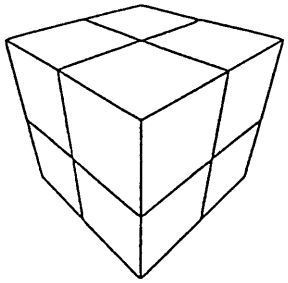

Figure – 8a Coarse Mesh – 27 Nodes

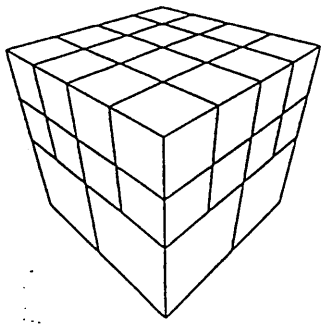

Figure – 8b I – Level Mesh with 84 Nodes

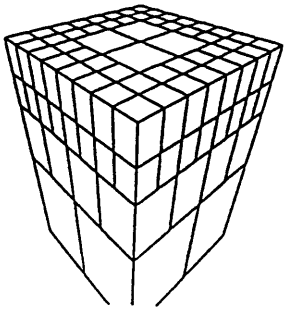

Figure – 8c II – Level Mesh with 252 Nodes

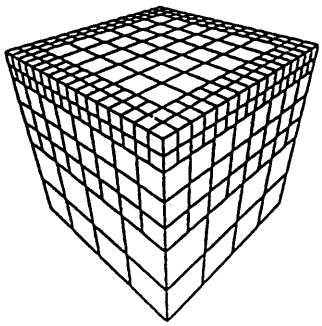

Figure – 8d III – Level Mesh with 898 Nodes

Figure 8 Sequence of 3D Adaptive Meshes for a Cube (Post-Processing Error Estimation Method).

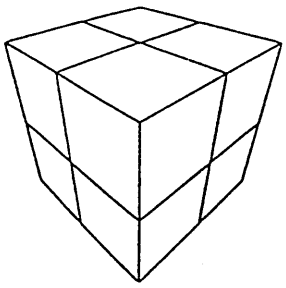

Figure – 9a Coarse Mesh – 27 Nodes

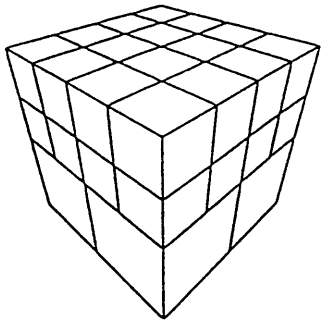

Figure – 9b I – Level Mesh with 84 Nodes

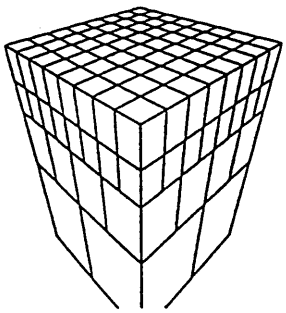

Figure – 9c II – Level Mesh with 277 Nodes

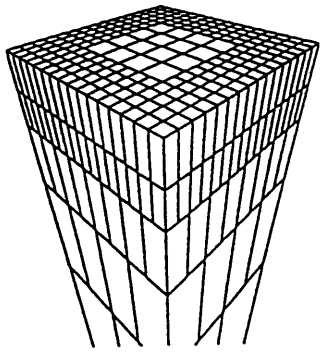

Figure – 9d III – Level Mesh with 853 Nodes

Figure 9 Sequence of 3D Adaptive Meshes for a Cube (Gradient Error Estimation Method).

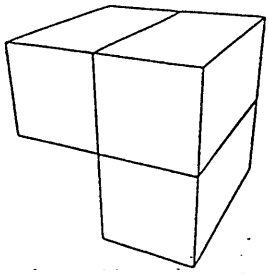

Figure – 10a Coarse Mesh – 16 Nodes

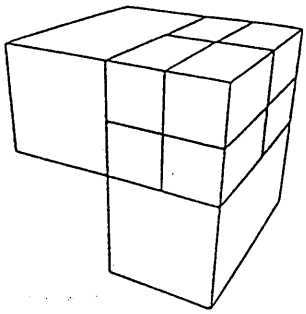

Figure – 10b I – Level Mesh with 35 Nodes

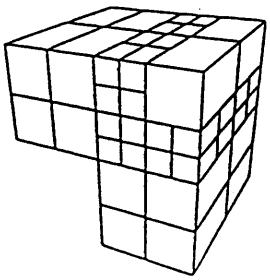

Figure – 10c II – Level Mesh with 144 Nodes

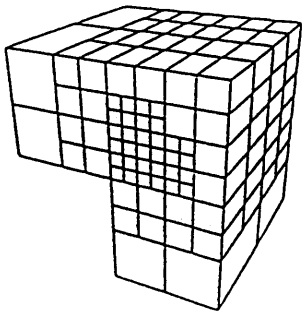

Figure – 10d III – Level Mesh with 604 Nodes

Figure 10 Sequence of Adaptive Meshes on a 3D L-Shaped Domain (Post-Processing Error Estimation Method).

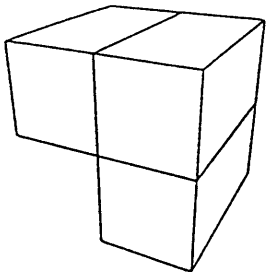

Figure – 11a Coarse Mesh – 16 Nodes

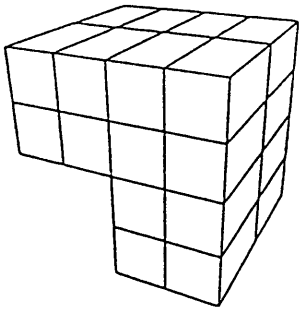

Figure – 11b I – Level Mesh with 63 Nodes

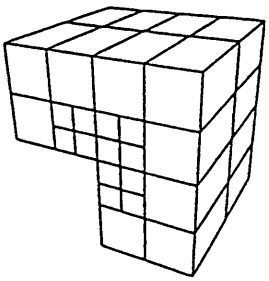

Figure – 11c II – Level Mesh with 144 Nodes

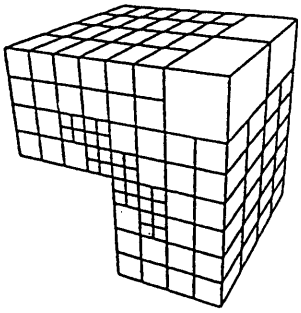

Figure – 11d III – Level Mesh with 582 Nodes

Figure 11 Sequence of Adaptive Meshes on a 3D L-Shaped Domain (Gradient Error Estimation Method).

there is a discontinuity which introduces more errors in the potential near the boundary than the other regions of the domain. As expected there are more refinements in the upper plane compared to other parts of the geometry. In the third level of refinement, the number of degrees of freedom is 898. However when the same problem was solved using the gradient of field method of error estimate, the corresponding level of accuracy was reached with 484 elements having 853 degrees of freedom for the same level of refinement. From the numerical results of the 3D problem, it can be concluded that the performance of the gradient of field method is better compared to the post-processing error estimate.

Both error estimates are also applied on a 3D L-section problem by imposing appropriate Dirichlet and Neumann boundary conditions. The corresponding adaptive meshes for the post-processing and the gradient of field methods are shown in Figures 10 and 11 respectively. The refinement is concentrated near the re-entrant corner of the 3D L-section as verified with its 2D counterpart. By comparing the two sets of adaptive mesh sequences for the same level of refinement, it can be concluded that the post-processing method needs more degrees of freedom than the gradient of field method to obtain the same accuracy. In the third level of refinement, the post-processing method generates 604 degrees of freedom whereas the gradient of field method needs only 582 degrees of freedom. Since at each level of mesh refinement, the post-processing method generates a mesh by the mesh halving procedure, it is computationally very expensive compared to the gradient of field method. On the other hand the gradient of field method can be easily formulated as a local problem and solved with fewer computational resources. The difference in their performance is due the fact that the rate of change or the variation of the gradient of the solution near the region of singularity is larger than the rate of change of the solution function itself. This behavior helps to identify the exact number of elements needed near a singular region to generate an optimal mesh.

VI CONCLUSIONS

Two different types of *'a posteriori'* error estimation strategies for adaptive mesh refinement were presented. The performance characteristics of both error estimates are verified by solving two electrostatic problems in 2D and 3D adaptively. A hierarchical minimal tree based algorithm is employed for generating a graded adaptive mesh. The numerical test results, the sequence of adaptive meshes and the flux plots established the effectiveness of the proposed error estimation strategies for adaptive mesh refinement. The higher element density of the mesh near the singular regions of the test problems indicates the acceptable performance of error indicators in steering the adaptive process. The numerical test results and the comparative analysis of the performance of error estimates allow us to conclude that the gradient of field method is simple to formulate and computationally less expensive and is efficient compared to the post-processing error estimate.

REFERENCES

1. Babuska, I. and Rheinboldt, W.C. "Adaptive approaches and reliability estimations in finite element analysis". *Comp. Methods in Applied Mech. and Eng.* pp. 519-540, (1979).

2. Babuska, I. and Miller, A. "The post-processing approach in the finite element method. part 3: *a posteriori* error estimates and adaptive mesh selection." *Int. J. Numer. Methods. Eng.* vol. **20**, pp. 2311-2324, (1984).
3. Babuska, I. and Rheinboldt, W.C. "*A posteriori* error estimates for the finite element method." *Int. J. Numer. Methods. Eng.* vol. **12**, pp. 1597-1615, (1978).
4. Carey, G.F. and Humphrey, D.L. "Mesh refinement and iterative solution methods for finite element computations." *Int. J. Numer. Methods. Eng.* vol. **17**, pp. 1717-1734, (1981).
5. Baehmann, P.L., Shephard, M.S. and Flaherty, J.E. "*A postriori* error estimation for triangular and tetrahedral quadratic elements using interior residuals." *Int. J. Numer. Methods. Eng.* vol. **34**, pp. 979-996, (1992).
6. Kelly, D.W., De, J.P., Gago, S.R. and Zienkiewicz, O.C. "*A-posteriori* error analysis and adaptive processes in the finite element method: part I-error analysis." *Int. J. Numer. Methods. Eng.* vol. **19**, pp. 1593-1619, (1983).
7. Zienkiewicz, O.C. and Zhu, J.Z. "The superconvergent patch recovery and *a posteriori* error estimates part 1: the recovery technique." *Int. J. Numer. Methods. Eng.* vol. **33**, pp. 1331-1364, (1992).
8. Zienkiewicz, O.C. and Zhu, J.Z. "The superconvergent patch recovery and *a posteriori* error estimates part 2: error estimates and adaptivity." *Int. J. Numer. Methods. Eng.* vol. **33**, pp. 1365-1382, (1992).
9. Zhu, J.Z. and Zienkiewicz, O.C. "Superconvergence recovery technique and a posteriori error estimators." *Int. J. Numer. Methods. Eng.* vol. **30**, pp. 1321-1339, (1990).
10. Ainsworth, M., Zhu, J.Z., Craig, A.W. and Zienkiewicz, O.C. "Analysis of the Zienkiewicz-Zhu *a posteriori* error estimator in the finite element method." *Int. J. Numer. Methods. Eng.* vol. **28**, pp. 2161-2174, (1989).
11. Eriksson, K., Johnson, C. "An adaptive finite element method for linear elliptic problems." *Mathematics of Computation.* vol. **50**, pp. 361-383, (1988).
12. Penman, J., Fraser, J.R., Smith, J.R. and Grieve, M.D. "Complementary energy methods in the computation of electrostatic fields." *IEEE Trans. on Magnetics.* vol. **Mag-19**, pp. 2288-2291, (1983).
13. Penman, J. and Fraser, J.R. "Dual and complementary energy methods in electromagnetism." *IEEE Trans. on Magnetics.* vol. **Mag-19**, pp. 2311-2316, (1983).
14. Kelly, D.W. "The self-equilibration of residuals and complementary *a posteriori* error estimates in the finite element method." *Int. J. Numer. Methods Eng.* vol. **20**, pp. 1491-1506, (1984).
15. Temam, R. *Numerical Analysis.* D. Reidel Publishing Company, Dordrecht-Holland, (1973).
16. Ciarlet, P.G. *The Finite Element Method for Elliptic Problems.* North-Holland Publishing Company, New York, (1978).
17. Chellamuthu, K.C. and Ida, N. "Algorithms and Data Structures for 2D and 3D Adaptive Finite Element Mesh Refinement." *Finite Elements in Analysis and Design.* vol. **17**, pp. 205-229, (1994).